ACS APPLIED MATERIALS & INTERFACES

Research Article

www.acsami.org

Molecular Size, Shape, and Electric Charges: Essential for Perylene Bisimide-Based DNA Intercalator to Localize in Cell Nuclei and Inhibit Cancer Cell Growth

Zejun Xu,[†] Wenyu Cheng,[†] Kunru Guo,[‡] Jieshi Yu,[‡] Jie Shen,*[,‡] Jun Tang,*[,‡] Wantai Yang,[†] and Meizhen Yin*[,†]

[†]State Key Laboratory of Chemical Resource Engineering, Key Laboratory of Carbon Fiber and Functional Polymers of Ministry of Education, Beijing Laboratory of Biomedical Materials, Beijing University of Chemical Technology, 100029 Beijing, China

[‡]State Key Laboratory of Agrobiotechnology and College of Veterinary Medicine, China Agricultural University, 100193 Beijing, China

Supporting Information

ABSTRACT: The molecular properties concerning size, shape, and electric charges of the planar aromatic DNA intercalators are still poorly understood. Herein, a series of water-soluble perylene bisimide (PBI) derivatives containing a rigid and planar aromatic nanoscaffold with different size, shape, and electric charges were synthesized. Using histochemistry and cell viability assays on animal tissues and cancer cells, we revealed the molecular properties required for successful DNA intercalators to localize in cell nuclei and inhibit cancer cells. Small molecular size and the strong polarity of hydrophilic substituents are prerequisites for PBI-based DNA intercalators. A large number of charges facilitate the nucleic accumulation of these DNA intercalators, while fewer charges and planar aromatic nanoscaffold more efficiently inhibit cancer cell growth.

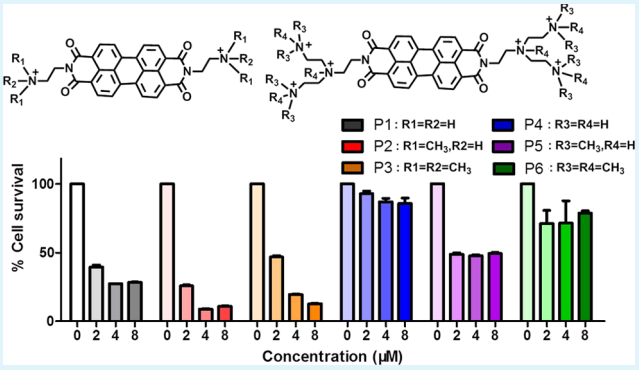

KEYWORDS: *perylene bisimide, DNA intercalator, cell imaging, nucleic accumulation, anticancer activity, planar aromatic nanoscaffold*

INTRODUCTION

Due to the outstanding chemical and photostability, the highly fluorescent perylene bisimides (PBIs) have been extensively studied as pigment colorants in nonpolar solvents for many years.[1−3] However, the lack of solubility of PBIs in polar solvents has impeded the utilization of PBIs in biological areas. To enhance the water solubility, hydrophilic functionalization in the bay region or at the imide positions of PBIs is required.[4−13] Water-soluble PBIs have attracted increasing attention in recent years for specific labeling and selective detection due to their stable fluorescence performance.[14−18] Recently, PBIs with large hydrophobic surfaces acting as either linker or surrogate base in artificial DNA have raised considerable concern.[19−21] The research of the above-mentioned PBIs−DNA hybrids has concentrated mostly on the cofacial $\pi-\pi$ stacking between G-quadruplexes and the planar structures of PBIs.[22,23] The noncovalent interactions between PBIs and DNA have seldom been reported. We previously developed a PBI-based DNA intercalator with high enrichment in cell nuclei that can inhibit cancer cell growth.[24] However, the molecular properties concerning size, shape, and electric charges of DNA intercalators are still poorly understood. Therefore, it would be of great interest to synthesize functional PBIs with different size, shape, and electric charges and to investigate their use as DNA intercalators and explore their cellular distribution and anticancer activity.

In this study, we designed and synthesized a series of water-soluble PBIs derivatives carrying amines either at the imide positions (**P1**−**P6**) or in the bay region (**P7**) (Scheme 1) to investigate their ability of intercalating into double-stranded DNA base pairs and the anticancer activity. The amines reported here involve primary amines (**P1** and **P4**), tertiary amines (**P2**, **P5**, and **P7**), and quaternized amines (**P3** and **P6**). **P4**, **P5**, and **P6** are the PBIs containing six amines at the imides positions, while **P1**, **P2**, and **P3** possess two amines. The nanosizes together with the planar structures are suitable to be used as DNA intercalators (Figure S1, Supporting Information). The results of histochemistry and cell viability assays on animal tissues and cancer cells demonstrated that PBI-based DNA intercalators toward localizing in cell nuclei and inhibiting

Received: February 22, 2015
Accepted: April 22, 2015
Published: April 22, 2015

DOI: 10.1021/acsami.5b01665
ACS Appl. Mater. Interfaces 2015, 7, 9784−9791

Scheme 1. Chemical Structures of Perylene Bisimides (PBIs) P1−P7 Containing Various Amines

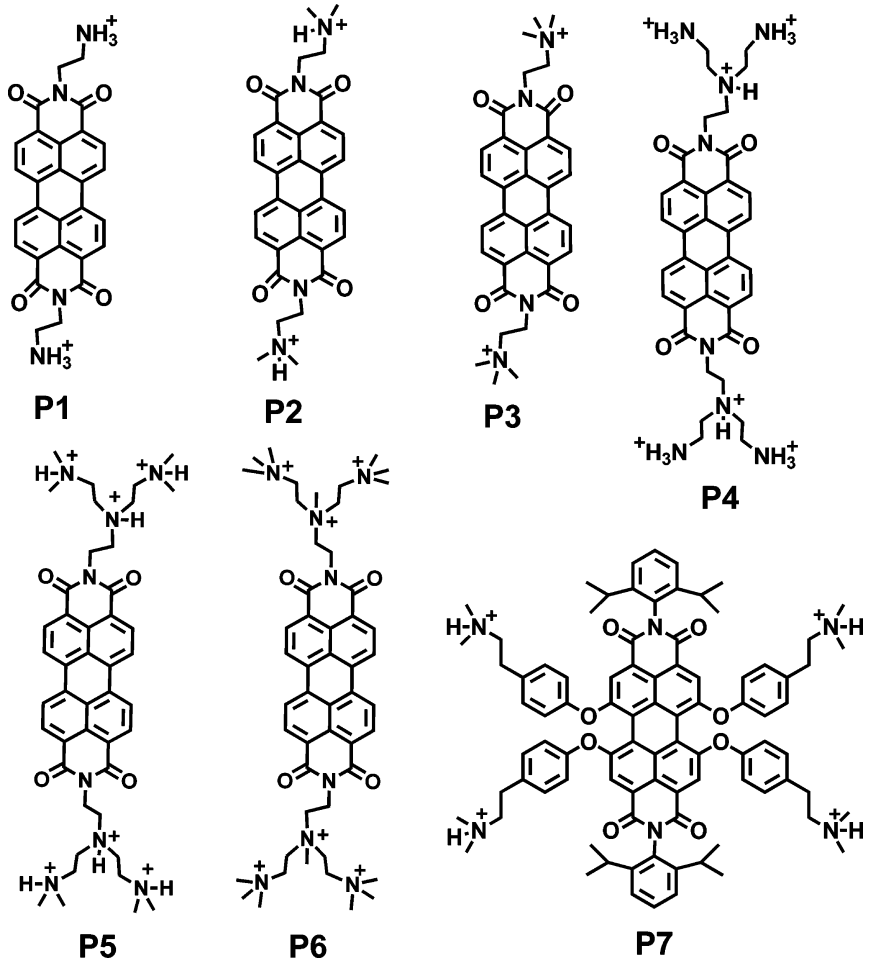

cancer cell growth required the special molecular characteristics, including small molecular size, strong polarity of hydrophilic substituents, planar shape, and appropriate number of charges.

EXPERIMENTAL SECTION

Material and Methods. 4-Methylbenzenesulfonic acid monohydrate (98.5%), *N,N′*-diethylethylenediamine (97%), triethylamine (Et_3N, 99.5%), methyl *p*-toluene sulfonate (98%), 2-(dimethylamino)-ethyl acrylate (98%), and tris(2-aminoethyl)amine (97%) were purchased from Alfa Aesar and used without further purification. Perylene-3,4,9,10-tetracarboxylic dianhydride (PBA) was received from Beijing Wenhaiyang perylene Chemistry (Beijing, China) and used directly. *tert*-Butyl (2-aminoethyl)carbamate was prepared according to the literature.[25] **P2** was produced as described previously.[24] All other reagents and solvents were purchased from commercial suppliers and were used as received. *Calf thymus* DNA (CT-DNA) was purchased from Sigma-Aldrich and used without further purification. A solution of CT-DNA in phosphate buffer (10 mM, pH 7.4) containing 50 mM NaCl was preserved at 4 °C and used within 4 days. The molar absorption coefficients of $\varepsilon_{260\ nm}$ = 6600 $M^{-1}cm^{-1}$ were adopted to determine the concentration of CT-DNA. The UV absorbance ratio at 260 and 280 nm is more than 1.8, indicating that the stock solution is free of protein.[24] Nuclear magnetic resonance (NMR) spectra were recorded on a Bruker 400 (400 MHz ^1H; 100 MHz ^{13}C) spectrometer using CF_3COOD as solvent at room temperature. Chemical shifts were reported downfield from 0.00 ppm using TMS as internal reference. The description of the signal fine structure means: s = singlet, d = doublet, br. s = broad signal, t = triplet, dt = doublet of triplet, q = quartet, tt = triplet of triplet, and m = multiplet. Matrix-assisted laser-desorption ionization time-of-flight mass spectrometry (MALDI-TOF MS) was determined on an AXIMA-CFR plus MALDI-TOF mass spectrometer. The spectrophotometer (Cintra 20, GBC, and Australia) was used to assay the UV−vis absorption spectra. Meanwhile, the fluorescence spectrophotometer (Horiba Jobin Yvon FluoroMax-4 NIR, NJ, USA) was used to study the fluorescence spectra at room temperature (25 °C). Fluorescence quantum yields were measured with cresyl violet in methanol as reference chromophore (the standard value is 0.54 in methanol) at room temperature.[5] A Jasco 810 spectropolarimeter was employed to record the circular dichroism (CD) spectra within a phosphate buffer (10 mM, pH 7.4) containing 50 mM NaCl. The Gaussian 09W software package was employed to calculate the geometry-optimized structure adopted by compounds **P1−P7** at the Ground state B3LYP/3-21G level.

UV−Vis Absorption and Emission Spectra Studies. The absorption and fluorescence spectroscopies of PBIs **P1−P7** were recorded at 25 °C in phosphate buffer (PBS, 10 mM, pH 7.4) containing 50 mM NaCl. The PBIs' optimum concentration was 5 μM in buffer. With the addition of double-stranded DNA, the changes of optical properties were recorded.

Circular Dichroism Spectra Studies. A Jasco 810 spectropolarimeter was employed to study the circular dichroism (CD) spectra at 25 °C in phosphate buffer (10 mM, pH 7.4) containing 50 mM NaCl. The CD spectral studies of double-stranded DNA (80 μM) with or without PBIs **P1−P7** (3 μM) were performed in phosphate buffer.

Viscosity Measurements. A Schott Viscosystem AVS 370 was employed to study the viscosity changes within phosphate buffer at 25 °C. CT-DNA was dissolved in phosphate buffer (10 mM, pH 7.4) containing 50 mM NaCl. The final base-pair concentration of CT-DNA was 50 μM. Ubbelodhe viscometer was employed to perform the

DOI: 10.1021/acsami.5b01665
ACS Appl. Mater. Interfaces 2015, 7, 9784−9791

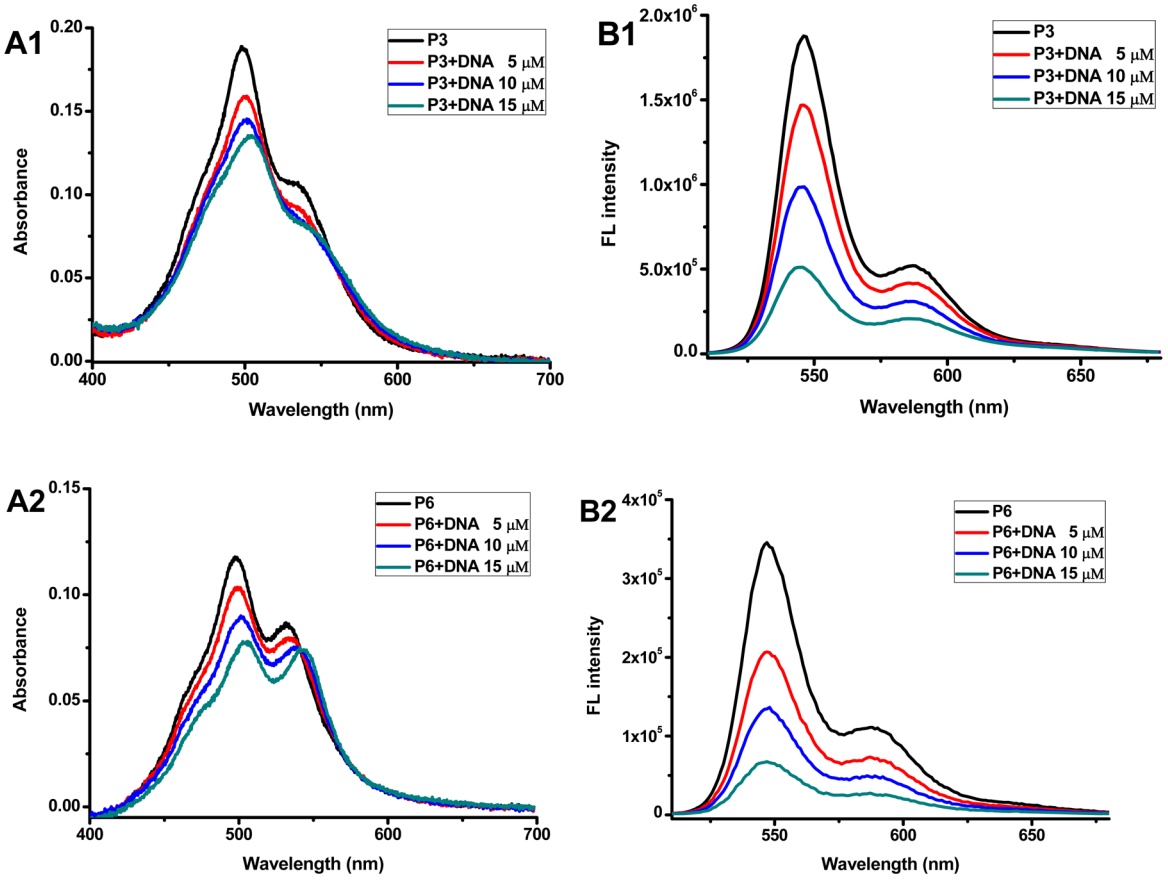

Figure 1. Absorbance and fluorescence intensity changes of **P3** (A1 and B1) and **P6** (A2 and B2) in phosphate buffer (10 mM, pH 7.4) containing 50 mM NaCl and double-stranded DNA at different base-pair concentrations (0 μM (black curve), 5 μM (red curve), 10 μM (blue curve), 15 μM (dark cyan curve)) at 25 °C with exposure to air (λ_{ex} = 498 nm).

viscometric titrations in a thermostated bath kept at room temperature. A digital stopwatch was used to record the flow times. Each sample was tested in triplicate, and the average flow time was calculated. Data is plotted as $(\eta/\eta^0)^{1/3}$ vs [complex]/[DNA]. η is the viscosity of the complex in buffer solution. Meanwhile, η^0 is the viscosity of CT-DNA in buffer solution alone. Viscosity values were calculated from the observed flowing time of DNA-containing solutions (t) corrected for that of the buffer alone (t_0), $\eta = (t - t_0)$.

Histochemical Staining. The histochemical studies were performed using different *Drosophila* larval tissues, including wing imaginal discs, haltere imaginal discs, leg imaginal discs, tracheal cells, salivary glands, and fat body. Only salivary glands are shown to compare the histochemical staining effects in this paper. After being dissected and fixed with 4% formaldehyde solution and 0.2% Triton-X100, the *Drosophila* third instar larvae were subsequently washed with PBS for 60 min. Dissected larvae were then incubated in 10 μM PBIs fluorescent compounds **P1**−**P7** for 60 min rotating at room temperature and finally washed with PBS for 60 min. The commercial nuclear dye 4′,6-diamidino-2-phenylindole (DAPI),[26] 1:500 (Sigma), was used to stain the cell nuclei. Images were taken with a Leica TCS SP2 AOBS confocal microscope.

Inhibition of Cancer Cells. MTT assays were adopted to evaluate the *in vitro* antiproliferative efficiencies of PBIs **P1**−**P7** against HeLa, HCT116, and S2 cells. MTT is a kind of water-soluble tetrazolium salt, and it can be transformed into colored but water-insoluble formazan crystals in living cells by mitochondrial dehydrogenases. 96-well dishes were employed to hold ten thousand cells, and then, the cells were incubated for 24 h. The tested compounds in water were then added, ranging from 0 to 8 μM. After 48 h of treatment, the MTT assay was adopted to evaluate the cell viability. Briefly, cells were cultivated with MTT solution (500 μg/mL) at 37 °C for 4 h. To replace MTT-containing medium, 150 μL of DMSO per well was added afterward. Shaking the dishes gently for 10 min dissolved the reaction product formazan salts. A microplate reader (Thermo Scientific Multiskan GO, Thermo Fisher Scicentific, Waltham, MA, USA) was adopted to measure the absorbance at a wavelength of 490 nm. Each of the experiments was repeated in triplicate. The cytotoxicity parameter IC_{50} is the concentration at which cell growth is inhibited by 50%. It was calculated by linear regression analysis of experimental data.

RESULTS

Synthesis of Perylene Bisimide-Based DNA Intercalators. As shown in Schemes 1 and S1−S3, Supporting Information, **P1**, **c**, and **P4** were efficiently obtained by a direct condensation of perylene-3,4,9,10-tetracarboxylicdianhydride (PBA) with ethane-1,2-diamine, *N*,*N*′-dimethylethane-1,2-diamine, and tris(2-aminoethyl)amine, respectively.[23] The two tertiary amines in compound **c** were treated with 4-methylbenzenesulfonic acid monohydrate and methyl *p*-toluene sulfonate in water at 50 °C to afford tertiary ammonium salt **P2** and quaternary ammonium salts **P3**, respectively.[24,27] The tertiary amination reaction of **P4** was performed with formaldehyde under excess formic acid to give their tertiary amine analogue **P5**. This is a classic Eschweiler-Clarke methylation that a primary (or secondary) amine is methylated into the tertiary amine using excess formic acid and formaldehyde.[28−31] The further quaterization of **P5** with methyl iodide yielded corresponding quaternary ammonium salts **P6**. Intermediate **d** bearing four primary amines in the bay region of PBI was synthesized according to the literature.[32] The tertiary amination of intermediate **d** was done by the above-

DOI: 10.1021/acsami.5b01665
ACS Appl. Mater. Interfaces 2015, 7, 9784−9791

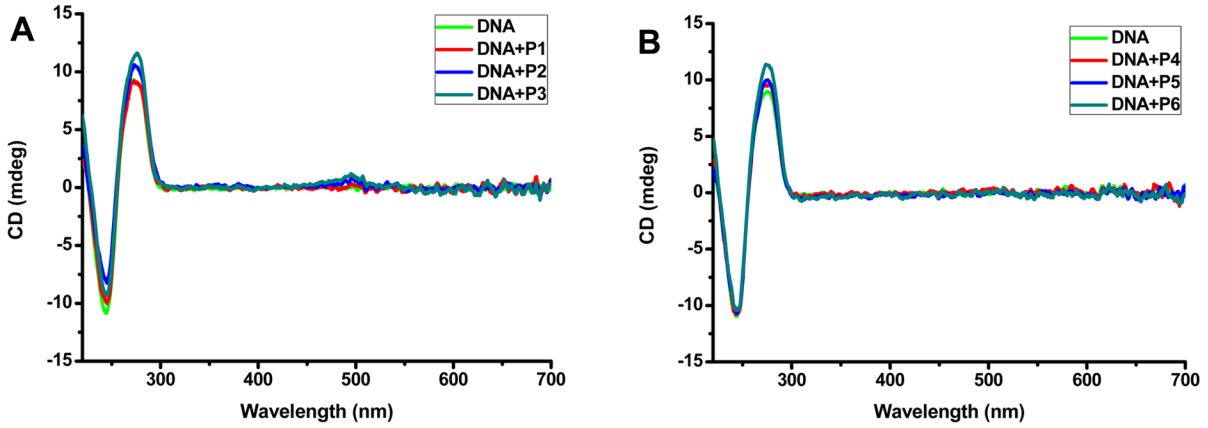

Figure 2. CD spectra of double-stranded DNA (base-pair concentration: 80 μM) in phosphate buffer (10 mM, pH 7.4) containing 50 mM NaCl with or without PBIs ((A) **P1**−**P3** and (B) **P4**−**P6**, 3 μM) at 25 °C.

mentioned classic Eschweiler-Clarke methylation to afford corresponding tertiary amine analogue **P7** (Scheme S4, Supporting Information). Finally, all the synthesized PBIs were fully characterized by NMR spectroscopy and MALDI-TOF mass spectrometry. The fluorescent quantum yields (FQYs) and water solubilities of these PBIs are given in Table S1, Supporting Information. In general, FQYs of quaternary ammonium salts (**P3** and **P6**) were higher than those of tertiary amine salts (**P2**, **P5**, and **P7**). FQYs of the PBIs bearing primary amines (**P1** and **P4**) are the weakest. The calculations of **P1**−**P7** sizes were performed using the Gaussian 09W Program upon energy minimization (Figure S1, Supporting Information). The length of perylene rigid planar scaffold of **P1**−**P6** is 1.15 nm, and the width of perylene scaffold is 0.49 nm (Figure S1A,B, Supporting Information). The sizes of **P7** are 1.86 × 0.48 × 1.7 nm (length × width × height) (Figure S1C, Supporting Information). **P7** possesses four quaternary ammonium salts in their bay region, which resulted in a nonplanar, twisted aromatic chromophore scaffold.[5]

Fluorescence Spectral Analysis of PBIs. The absorption spectroscopies of PBIs **P1**, **P2**, and **P3** that contain two amines at the imide positions were first studied. With the addition of DNA, the absorption spectra of PBIs **P1**, **P2**, and **P3** show gradual hypochromicity accompanied by a slight red shift of the absorption maximum at 498 nm (Figures S2A1,A2, Supporting Information, and 1A). These spectral characteristics show a reduction in the $\pi \rightarrow \pi^*$ promoting energy which is attributed to strong π stacking between the intercalating ligand of an aromatic chromophore and the base pairs of DNA. When DNA concentration reached 15 μM, the PBIs **P1**, **P2**, and **P3** displayed hypochromicity of 24.1%, 26.9%, and 28.3%, and the red-shifted absorption maxima were read as 5, 5, and 7 nm in comparison with that of the free ones, respectively. Interestingly, one isosbestic point was observed at 554 nm for **P2** and **P3**. The absorption spectroscopies of PBIs **P4**, **P5**, and **P6** that contain six amines at the imides were investigated as well. The addition of DNA into the solution of PBIs **P4**, **P5**, and **P6** induces gradual hypochromicity and slight bathochromic shift in absorption maximum (Figures S2A3,A4, Supporting Information, and 1A2). At a DNA concentration of 15 μM, a substantial hypochromicity (15.3% for **P4**, 25.7% for **P5**, and 33.7% for **P6**) in absorption maximum occurs accompanied by an apparent bathochromic shift (6 nm for **P4** and 7 nm for both PBIs **P5** and **P6**). Subsequently, the addition of DNA into the solution of **P7** does not lead to an obvious change in the absorption spectra (Figure S2A5, Supporting Information).

Next, the fluorescent properties of PBIs **P1**−**P7** were measured in the above-mentioned buffer at 25 °C. As shown in Figures 1B1,B2 and S2B1−B4, Supporting Information, the fluorescence spectra of **P1**−**P6** show a narrow peak at 580 nm (half bandwidth: 10 nm) and a broad peak around 545 nm (half bandwidth: 25 nm). Upon addition of DNA, the fluorescence intensities of PBIs **P1**−**P6** gradually decrease accompanied by ∼2 nm blue shifts at the fluorescence peaks. In the case of **P7**, the emission maximum is around 630 nm and the fluorescent intensities gradually and slightly decrease with the addition of DNA (Figure S2B5, Supporting Information). These data suggest that PBIs **P1**−**P6** can serve as DNA-intercalating agents.[24,33,34]

Circular Dichroism (CD) Spectral Analysis of PBIs. When the interaction occurs among small-size molecules and DNA, CD spectral analysis will be a suitable method to detect the conformational changes of DNA morphology. CD spectrum of pure DNA (green curve, Figure 2A) shows a positive band at 277 nm (base staking) and a negative band at 247 nm (polynucleotide helicity).[24,35,36] As can be seen in Figure 2A, upon the addition of PBIs **P1**, **P2**, and **P3** into the DNA buffer, there is an increase in the intensities of positive band at 277 nm but a decrease of negative band at 247 nm. One more valuable phenomenon is that a weak positive induced CD (ICD) signal can be observed at ∼500 nm due to the absorption of perylene bisimide. However, the intensity of the positive band at 277 nm increases slightly after addition of **P1** (red curve, Figure 2A). The peak level at 277 nm induced by **P3** (dark cyan curve, Figure 2A) is higher than that induced by **P2** (blue curve, Figure 2A). Next, the CD spectroscopies of PBIs **P4**, **P5**, and **P6** with double-stranded DNA were investigated. Upon the addition of PBIs **P4**, **P5**, and **P6** into the DNA buffer, the intensities of the positive band at 277 nm increase, while the intensities of the negative band at 247 nm do not change (Figure 2B). The peak level at 277 nm induced by **P6** (dark cyan curve, Figure 2B) is higher than that induced by **P5** (blue curve, Figure 2B) and **P4** (red curve, Figure 2B). On the contrary, the addition of **P7** into the DNA buffer does not lead to an obvious change in CD spectra (Figure S3, Supporting Information). These data indicate that PBIs **P1**−**P6** have DNA-intercalation ability.[24]

Viscosity Assays of PBI−DNA Complexes. The most efficient parameter to evaluate the binding mode between PBI

DOI: 10.1021/acsami.5b01665
ACS Appl. Mater. Interfaces 2015, 7, 9784−9791

and DNA is the viscosity of the PBI–DNA complex.[37,38] Intercalators dramatically increase the length of DNA, leading to the increasing viscosity. In contrast, a groove binder or electrostatic interaction does not lengthen the DNA helix and thus does not increase the viscosity of DNA solutions.[39] On the basis of the mechanism mentioned above, the binding modes between PBIs **P1**–**P7** and DNA are evaluated by viscosity assays. As shown in Figure 3, the increasing viscosities of PBIs

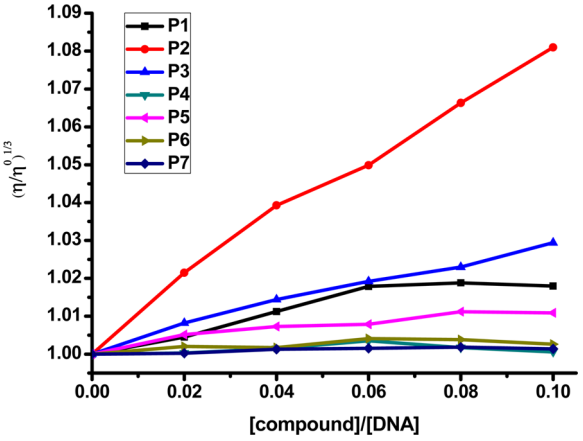

Figure 3. Effect of increasing amounts of PBIs **P1**–**P7** on the relative viscosities of CT-DNA (base-pair concentration of DNA: [DNA] = 50 μM) at room temperature. η is the viscosity of DNA in the presence of the compounds, and η^0 is the viscosity of DNA in the absence of the PBIs.

P1–**P3** and **P5**/DNA complexes follow the rising ratio of [compound]/[DNA], while the viscosities of PBIs **P4**, **P6**, and **P7**/DNA complexes do not change along with the ratio of [compound]/[DNA]. These results suggest that PBIs **P1**–**P3** and **P5** are effective DNA intercalators.

Visualization of the Cellular Distribution of PBIs. Subsequently, the cellular distribution of PBIs **P1**–**P7** is monitored within animal tissues. In the staining of different *Drosophila* larval tissues, **P2**, **P3**, **P5**, and **P6** were both exclusively localized in the cell nuclei in all tested tissues, while **P1** did not show any specific distribution in cells (Figures 4 and 5). The DNA staining effects of **P2** in some tissues are worse than those of **P3** (Figure 4). Meanwhile, the DNA staining effects of **P6** in some tissues are better than those of **P5** (Figure 5). **P7** cannot specifically label cell nucleus (Figure S6, Supporting Information). These data suggest that smaller size and stronger charges of PBIs can facilitate PBI-nucleic enrichment. Therefore, **P1**–**P6** have the potential to be further explored as anticancer drugs.

Anticancer Cells Assays. We then examined the inhibitory effect of PBIs **P1**–**P7** on two human cancer lines HeLa and HCT116 by using the 3-(4,5-dimethylthiazolyil-2)-2,5-diphenyltetrazolium bromide (MTT) assay.[40] As shown in Figure 6, PBIs **P1**, **P2**, and **P3** had good anticancer activity against cancer cell lines with an IC_{50} value lower than 2.0 μM. PBIs **P4**, **P6**, and **P7** exhibited weak anticancer activity, while **P5** showed moderate anticancer activity (Figures 6 and S7 and S8, Supporting Information). When applied to noncancer cells (S2 cells), **P1**–**P7** showed relatively lower cytotoxicity (Figure S9, Supporting Information).These data suggest that stronger charges of PBIs restrict their anticancer ability.

DISCUSSION

In order to investigate the molecular properties that influence PBI-based DNA intercalator candidates toward localizing in cell nuclei and inhibiting cancer cell growth, we designed and synthesized PBI derivatives carrying various amines either at the imide positions (**P1**–**P6**) or in the bay region (**P7**) (Scheme 1). These PBIs can be classified to compare their effects on cell nuclei distribution and anticancer ability. **P1**–**P6** are smaller and planar-shaped vs **P7**. **P1**–**P3** contain a fewer number of amines than **P4**–**P6**.

The large size and nonplanar shape of **P7** interfere with the intercalation. As discussed in the literature,[24,41,42] significant hypochromicity accompanied by a slight red shift phenomenon exhibited by compound/DNA complexes suggest a classical DNA intercalation of PBIs **P1**–**P6** into DNA. Increasing the amount of DNA causes the decrease of fluorescence intensities and a slight blue shift in the emission maximum of **P1**–**P6** (Figures 1B1,B2 and S2B1–B4, Supporting Information). These fluorescence changes are consistent with the optical properties of DNA intercalators reported in the literature.[24,33,34] The fluorescence change of **P7** can be attributed to the electrostatic interaction between the positive charges of **P7** and the alternating phosphate groups of DNA backbones. Therefore, **P7** can not serve as DNA-intercalating agent.

Because of the symmetry of PBI derivatives, they are not optically active. The CD spectroscopies (Figure 2) of **P1**–**P3**/DNA exhibit an increase at 277 nm and decrease at 247 nm, suggesting that PBIs **P1**, **P2**, and **P3** intercalate into the space between two adjacent base pairs of DNA and affect the stability of DNA helix. The increase of the positive peak at 277 nm and the decrease of the negative peak at 247 nm verified that the DNA conformation changed from the B-form to the A-

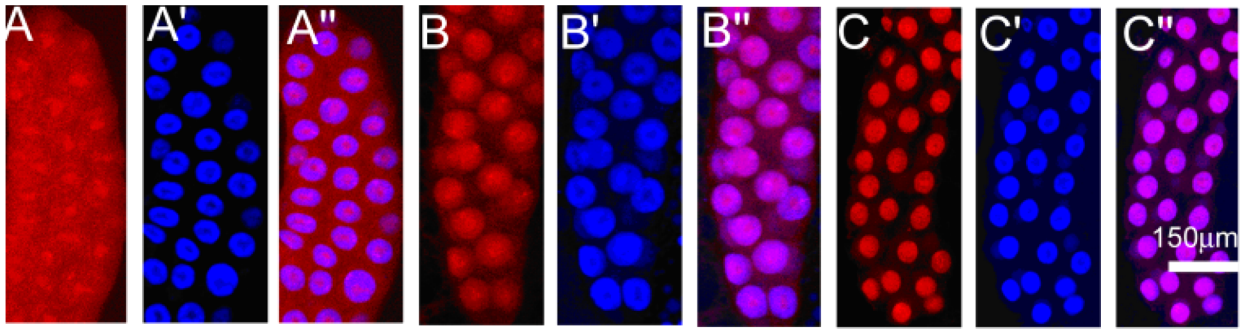

Figure 4. Fluorescence images of salivary glands incubated with (A, B, and C) **P1**, **P2**, and **P3** (red), (A′, B′, and C′) DAPI (blue), and (A″, B″, and C″) merged channels of **P1**–**P3** and DAPI.

DOI: 10.1021/acsami.5b01665
ACS Appl. Mater. Interfaces 2015, 7, 9784–9791

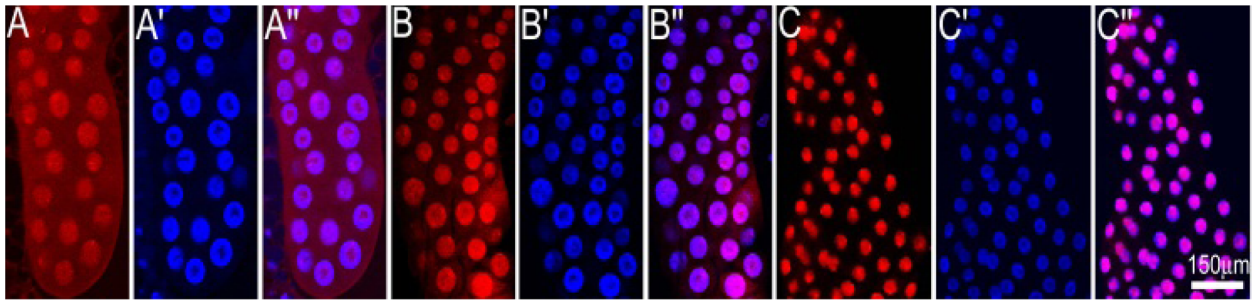

Figure 5. Fluorescence images of salivary glands incubated with (A, B, and C) PBIs **P4**, **P5**, and **P6** (red), (A′, B′, and C′) DAPI (blue), and (A″, B″, and C″) merged channels of PBIs **P4**−**P6** and DAPI.

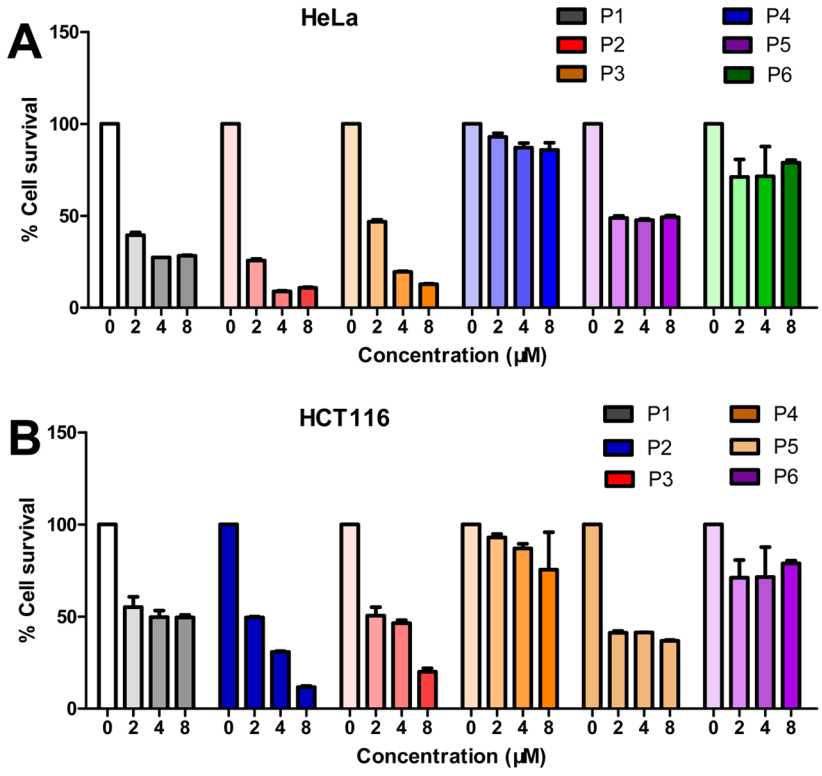

Figure 6. MTT assays of (A) HeLa and (B) HCT116 cells incubated with PBIs **P1**−**P6** for 48 h, and the concentration of PBIs **P1**−**P6** increased from 0 to 8 μM.

form.[41,40] Meanwhile, the weak positive ICD indicates that PBIs **P1**, **P2**, and **P3** can efficiently intercalate into the base pairs of double-stranded DNA.[24] According to the changes in CD spectra, we conclude that the DNA-intercalating ability of PBIs follows the order: **P3** > **P2** ≫ **P1**. PBIs **P4**−**P6** only cause the increase in positive band at 277 nm but do not influence the negative one at 247 nm in CD spectra, indicating that **P4**−**P6** have compromised intercalation ability (**P6** > **P5** > **P4**) and do not affect the DNA helix. As expected, **P7** can not intercalate into double-stranded DNA (Figure S3, Supporting Information).

The viscosities of **P1**−**P7**/DNA complexes were investigated to reveal the binding mode between compounds and DNA (Figure 3). The viscosity values increase by increasing the ratio of [compound]/[DNA] for **P1**−**P3** but not for **P4**−**P6**. This is the unique characteristic of the intercalation mechanism.[24,43] Among them, **P2** shows the highest signal which implies that the distances between adjacent base pairs of DNA are mostly lengthened. Therefore, moderate charges of PBIs are more suitable for intercalative interaction with DNA.

On the basis of the results of absorption, emission, CD spectroscopic studies, and viscosity measurements, we can conclude that the intercalation ability of PBIs into DNA follows the order: **P1**−**P3** ≫ **P4**−**P6**. However, due to the nonplanner structure, **P7** can not intercalate into the base pairs of double-stranded DNA.

For *in vitro* experiments on cell and tissue levels, nucleic enrichment would facilitate a drug to intercalate into DNA and inhibit the growth of cancer cells. Due to the fluorescence characteristic of PBIs, the cellular distribution of PBIs derivatives **P1**−**P7** was visualized under the fluorescence microscope. PBIs **P1**−**P6** have different abilities to be enriched in cell nuclei in all tested tissues (Figures 4 and 5). Among them, PBIs with more charges have better nucleic distribution than those with fewer charges. The electrostatic interaction between PBIs and nuclei acid plays a predominant role for their

DOI: 10.1021/acsami.5b01665
ACS Appl. Mater. Interfaces 2015, 7, 9784−9791

nucleic enrichment. This is the reason that the PBIs with strong charges show good nucleic enrichment.

For anticancer activity, efficiencies of both DNA intercalation and nuclei distribution are important. As expected, PBIs **P1**−**P3** are good DNA intercalators, and they show good abilities in the suppression of cancer cell growth (Figure 6). **P5** only has an intermediate inhibition effect on cancer cells (Figure 6), which is consistent with its relatively high value in DNA viscosity assay (Figure 3).

CONCLUSION

In conclusion, we have developed a series of PBI derivatives with various hydrophilic substituents and molecular sizes as well as shapes. Absorption, emission, and CD spectral analyses as well as viscosity measurements were used to investigate the DNA intercalation properties of PBI derivatives. The spectral analyses and viscosity measurements demonstrated that PBIs **P1**−**P3** and **P5** serve as effective DNA intercalating agents, while **P4** and **P6** interact with DNA through both intercalative and electrostatic interaction modes. These results suggest that PBIs derivatives serving as good DNA intercalator should possess planar scaffold, small molecular size, the stronger polarity of hydrophilic substituents, and moderate charges. The cellular distribution results suggest that PBIs **P2**, **P3**, **P5**, and **P6** can specifically accumulate in the cell nuclei of animal tissues by intercalation and electrostatic interaction with DNA, while the nuclear accumulation effects of PBIs **P5** and **P6** in some tissues are better than that of **P2** and **P3**, due to the larger number of charges and better water solubility of **P5** and **P6**. Furthermore, the anticancer activity of these agents is mainly dependent on the moderate charge numbers and planar aromatic nanoscaffold. Consistently, PBIs **P2** and **P3** show the best performance in anticancer assays. Our work reveals the molecular prerequisites for efficient design of anticancer drugs.

ASSOCIATED CONTENT

Supporting Information

Synthesis of fluorescent perylene amine derivates, UV/vis absorption and fluorescence emission properties. The Supporting Information is available free of charge on the ACS Publications website at DOI: 10.1021/acsami.5b01665.

AUTHOR INFORMATION

Corresponding Authors

*E-mail: shenjie@cau.edu.cn.
*E-mail: jtang@cau.edu.cn.
*E-mail: yinmz@mail.buct.edu.cn.

Notes

The authors declare no competing financial interest.

ACKNOWLEDGMENTS

This work was financially supported by the National Natural Science Foundation of China (21174012, 51103008, 51221002), the 973 Program (2013CB127603), the Project for Extramural Scientists of State Key Laboratory of Agrobiotechnology (2015SKLAB6-22), and the Beijing Natural Science Foundation (2142026).

REFERENCES

(1) Kazmaier, P. M.; Hoffmann, R. A Theoretical Study of Crystallochromy. Quantum Interference Effects in the Spectra of Perylene Pigments. *J. Am. Chem. Soc.* **1994**, *116*, 9684−9691.
(2) Würthner, F. Perylene Bisimide Dyes as Versatile Building Blocks for Functional Supramolecular Architectures. *Chem. Commun.* **2004**, 1564−1579.
(3) Zhu, L.; Wu, W.; Zhu, M.-Q.; Han, J. J.; Hurst, J. K.; Li, A. D. Q. Reversibly Photoswitchable Dual-Color Fluorescent Nanoparticles as New Tools for Live-Cell Imaging. *J. Am. Chem. Soc.* **2007**, *129*, 3524−3526.
(4) Backes, C.; Schmidt, C. D.; Hauke, F.; Boettcher, C.; Hirsch, A. High Population of Individualized SWCNTs through the Adsorption of Water-Soluble Perylenes. *J. Am. Chem. Soc.* **2009**, *131*, 2172−2184.
(5) Kohl, C.; Weil, T.; Qu, J.; Müllen, K. Towards Highly Fluorescent and Water-Soluble Perylene Dyes. *Chem.−Eur. J.* **2004**, *10*, 5297−5310.
(6) Qu, J. Q.; Kohl, C.; Pottek, M.; Müllen, K. Ionic Perylenetetracarboxdiimides: Highly Fluorescent and Water-Soluble Dyes for Biolabeling. *Angew. Chem., Int. Ed.* **2004**, *43*, 1528−1531.
(7) Rehm, S.; Stepanenko, V.; Zhang, X.; Rehm, T. H.; Würthner, F. Spermine-Functionalized Perylene Bisimide Dyes-Highly Fluorescent Bola-Amphiphiles in Water. *Chem.−Eur. J.* **2010**, *16*, 3372−3382.
(8) Schmidt, C. D.; Boettcher, C.; Hirsch, A. Synthesis and Aggregation Properties of Water-Soluble Newkome-Dendronized Perylenetracarboxdiimides. *Eur. J. Org. Chem.* **2007**, 5497−5505.
(9) Gorl, D.; Zhang, X.; Würthner, F. Molecular Assemblies of Perylene Bisimide Dyes in Water. *Angew. Chem., Int. Ed.* **2012**, *51*, 6328−6348.
(10) Heek, T.; Fasting, C.; Rest, C.; Zhang, X.; Würthner, F.; Haag, R. Highly Fluorescent Water-Soluble Polyglycerol-Dendronized Perylene Bisimide Dyes. *Chem. Commun.* **2010**, *46*, 1884−1886.
(11) Rehm, T. H.; Stojkovic, M. R.; Rehm, S.; Skugor, M.; Piantanida, I.; Würthner, F. Interaction of Spermine-Alanine Functionalized Perylene Bisimide Dye Aggregates with ds-DNA/RNA Secondary Structure. *Chem. Sci.* **2012**, *3*, 3393−3397.
(12) Zhong, L.; Xing, F.; Shi, W.; Yan, L.; Xie, L.; Zhu, S. Synthesis, Spectra, and Electron-Transfer Reaction of Aspartic Acid-Functionalized Water-Soluble Perylene Bisimide in Aqueous Solution. *ACS Appl. Mater. Interfaces* **2013**, *5*, 3401−3407.
(13) Feng, X.; An, Y.; Yao, Z.; Li, C.; Shi, G. A Turn-On Fluorescent Sensor for Pyrophosphate Based on the Disassembly of Cu^{2+}-Mediated Perylene Diimide Aggregates. *ACS Appl. Mater. Interfaces* **2012**, *4*, 614−618.
(14) Peneva, K.; Mihov, G.; Herrmann, A.; Zarrabi, N.; Boersch, M.; Duncan, T. M.; Müllen, K. Exploiting the Nitrilotriacetic Acid Moiety for Biolabeling with Ultrastable Perylene Dyes. *J. Am. Chem. Soc.* **2008**, *130*, 5398−5399.
(15) Peneva, K.; Mihov, G.; Nolde, F.; Rocha, S.; Hotta, J.-i.; Braeckmans, K.; Hofkens, J.; Uji-i, H.; Herrmann, A.; Müllen, K. Water-Soluble Monofunctional Perylene and Terrylene Dyes: Powerful Labels for Single-Enzyme Tracking. *Angew. Chem., Int. Ed.* **2008**, *47*, 3372−3375.
(16) Yang, S. K.; Shi, X.; Park, S.; Doganay, S.; Ha, T.; Zimmerman, S. C. Monovalent, Clickable, Uncharged, Water-Soluble Perylenediimide-Cored Dendrimers for Target-Specific Fluorescent Biolabeling. *J. Am. Chem. Soc.* **2011**, *133*, 9964−9967.
(17) Yin, M.; Ding, K.; Gropeanu, R. A.; Shen, J.; Berger, R.; Weil, T.; Müllen, K. Dendritic Star Polymers for Efficient DNA Binding and Stimulus-Dependent DNA Release. *Biomacromolecules* **2008**, *9*, 3231−3238.
(18) Yin, M.; Shen, J.; Gropeanu, R.; Pflugfelder, G. O.; Weil, T.; Müllen, K. Fluorescent Core/Shell Nanoparticles for Specific Cell-Nucleus Staining. *Small* **2008**, *4*, 894−898.
(19) Neelakandan, P. P.; Pan, Z.; Hariharan, M.; Zheng, Y.; Weissman, H.; Rybtchinski, B.; Lewis, F. D. Hydrophobic Self-Assembly of a Perylenediimide-Linked DNA Dumbbell into Supramolecular Polymers. *J. Am. Chem. Soc.* **2010**, *132*, 15808−15813.
(20) Häner, R.; Biner, S. M.; Langenegger, S. M.; Meng, T.; Malinovskii, V. L. A Highly Sensitive, Excimer-Controlled Molecular Beacon. *Angew. Chem., Int. Ed.* **2010**, *49*, 1227−1230.
(21) Teo, Y. N.; Kool, E. T. DNA-Multichromophore Systems. *Chem. Rev.* **2012**, *112*, 4221−4245.

DOI: 10.1021/acsami.5b01665
ACS Appl. Mater. Interfaces 2015, 7, 9784−9791

(22) Micheli, E.; D'Ambrosio, D.; Franceschin, M.; Savino, M. Water Soluble Cationic Perylene Derivatives as Possible Telomerase Inhibitors: The Search for Selective G-Quadruplex Targeting. *Mini-Rev. Med. Chem.* **2009**, *9*, 1622−1632.
(23) Tuntiwechapikul, W.; Taka, T.; Bethencourt, M.; Makonkawkeyoon, L.; Lee, T. R. The Influence of pH on the G-Quadruplex Binding Selectivity of Perylene Derivatives. *Bioorg. Med. Chem. Lett.* **2006**, *16*, 4120−4126.
(24) Xu, Z.; Guo, K.; Yu, J.; Sun, H.; Tang, J.; Shen, J.; Müllen, K.; Yang, W.; Yin, M. A Unique Perylene-Based DNA Intercalator: Localization in Cell Nuclei and Inhibition of Cancer Cells and Tumors. *Small* **2014**, *10*, 4087−4092.
(25) Schneider, R. L.; Schmitt, F.; Frochot, C.; Fort, Y.; Lourette, N.; Guillemin, F.; Muller, J. F.; Barberi-Heyob, M. Design, Synthesis, and Biological Evaluation of Folic Acid Targeted Tetraphenylporphyrin as Novel Photosensitizers for Selective Photodynamic Therapy. *Bioorg. Med. Chem.* **2005**, *13*, 2799−2808.
(26) Qu, W.; Chen, S.; Ren, S.; Jiang, X.-j.; Zhuo, R.-x.; Zhang, X.-z. A Bioreducible Polypeptide for Efficient Gene Transfection Both *in Vitro* and *in Vivo*. *Chin. J. Polym. Sci.* **2013**, *31*, 713−718.
(27) Tam-Chang, S.-W.; Helbley, J.; Iverson, I. K. A Study of the Structural Effects on the Liquid-Crystalline Properties of Ionic Perylenebis(dicarboximide)s Using UV-Vis Spectroscopy, Polarized Light Microscopy, and NMR Spectroscopy. *Langmuir* **2008**, *24*, 2133−2139.
(28) Ciampolini, M.; Nardi, N. Five-Coordinated High-Spin Complexes of Bivalent Cobalt, Nickel, and Copper with Tris(2-dimethylaminoethyl)amine. *Inorg. Chem.* **1966**, *5*, 41−44.
(29) Clarke, H. T.; Gillespie, H. B.; Weisshaus, S. Z. The Action of Formaldehyde on Amines and Amino Acids. *J. Am. Chem. Soc.* **1933**, *55*, 4571−4587.
(30) Farkas, E.; Sunman, C. J. Chiral Synthesis of Doxpicomine. *J. Org. Chem.* **1985**, *50*, 1110−1112.
(31) Pine, S. H.; Sanchez, B. L. Formic Acid-Formaldehyde Methylation of Amines. *J. Org. Chem.* **1971**, *36*, 829−832.
(32) Klok, H. A.; Hernandez, J. R.; Becker, S.; Müllen, K. Star-Shaped Fluorescent Polypeptides. *J. Polym. Sci. Part A: Polym. Chem.* **2001**, *39*, 1572−1583.
(33) Plsikova, J.; Janovec, L.; Koval, J.; Ungvarsky, J.; Mikes, J.; Jendzelovsky, R.; Fedorocko, P.; Imrich, J.; Kristian, P.; Kasparkova, J.; Brabec, V.; Kozurkova, M. 3,6-Bis(3-alkylguanidino)acridines as DNA-Intercalating Antitumor Agents. *Eur. J. Med. Chem.* **2012**, *57*, 283−295.
(34) Xie, L.; Cui, J.; Qian, X.; Xu, Y.; Liu, J.; Xu, R. 5-Non-amino Aromatic Substituted Naphthalimides as Potential Antitumor Agents: Synthesis via Suzuki Reaction, Antiproliferative Activity, and DNA-Binding Behavior. *Bioorg. Med. Chem.* **2011**, *19*, 961−967.
(35) Jiang, X.; Shang, L.; Wang, Z. X.; Dong, S. J. Spectrometric and Voltammetric Investigation of Interaction of Neutral Red with Calf Thymus DNA: pH Effect. *Biophys. Chem.* **2005**, *118*, 42−50.
(36) Li, X.; Lin, Y.; Wang, Q.; Yuan, Y.; Zhang, H.; Qian, X. The Novel Anti-tumor Agents of 4-Triazol-1,8-naphthalimides: Synthesis, Cytotoxicity, DNA Intercalation and Photocleavage. *Eur. J. Med. Chem.* **2011**, *46*, 1274−1279.
(37) Graves, D. E.; Velea, L. M. Intercalative Binding of Small Molecules to Nucleic Acids. *Curr. Org. Chem.* **2000**, *4*, 915−929.
(38) Long, E. C.; Barton, J. K. On Demonstrating DNA Intercalation. *Acc. Chem. Res.* **1990**, *23*, 271−273.
(39) Inclan, M.; Albelda, T.; Frias, J. C.; Blasco, S.; Verdejo, B.; Serena, C.; Salat-Canela, C.; Luisa Diaz, M.; Garcia-Espana, A.; Garcia-Espana, E. Modulation of DNA Binding by Reversible Metal-Controlled Molecular Reorganizations of Scorpiand-like Ligands. *J. Am. Chem. Soc.* **2012**, *134*, 9644−9656.
(40) Chen, Z.; Liang, X.; Zhang, H.; Xie, H.; Liu, J.; Xu, Y.; Zhu, W.; Wang, Y.; Wang, X.; Tan, S.; Kuang, D.; Qian, X. A New Class of Naphthalimide-Based Antitumor Agents That Inhibit Topoisomerase II and Induce Lysosomal Membrane Permeabilization and Apoptosis. *J. Med. Chem.* **2010**, *53*, 2589−2600.
(41) Zhang, Z.; Yang, Y.; Zhang, D.; Wang, Y.; Qian, X.; Liu, F. Acenaphtho [1,2-b] Pyrrole Derivatives as New Family of Intercalators: Various DNA Binding Geometry and Interesting Antitumor Capacity. *Bioorg. Med. Chem.* **2006**, *14*, 6962−6970.
(42) Wang, K. R.; Wang, Y. Q.; Yan, X. H.; Chen, H.; Ma, G.; Zhang, P. Z.; Li, J. M.; Li, X. L.; Zhang, J. C. DNA Binding and Anticancer Activity of Naphthalimides with 4-Hydroxyl-Alkylamine Side Chains at Different Lengths. *Bioorg. Med. Chem. Lett.* **2012**, *22*, 937−941.
(43) Ihmels, H.; Otto, D. Intercalation of Organic Dye Molecules into Double-Stranded DNA−General Principles and Recent Developments. *Top. Curr. Chem.* **2005**, *258*, 161−204.

DOI: 10.1021/acsami.5b01665
ACS Appl. Mater. Interfaces 2015, 7, 9784−9791